Axial Symmetric Solutions of the Linear Sigma Model

D. Urbano[a)], A. Silva[b)], M. Fiolhais[b)] and P. Alberto[b)]

[a)] *Faculdade de Engenharia da Universidade do Porto, P-4000 Porto, Portugal*

[b)] *Departamento de Física da Universidade and Centro de Física Teórica P-3000 Coimbra, Portugal*

Received March 25, 1996

Solitonic solutions with axial symmetry (in configuration and isospin spaces) are studied in the framework of the linear sigma model with quarks, σ and π mesons. A comparison between the axial and the hedgehog solitons is presented in detail. It turns out that the axial soliton is less bound than the hedgehog. States with good angular momentum and isospin are extracted from the axial state by means of the Peierls-Yoccoz projection. The relevance of the axial ansatz is discussed in the context of a description of the angular momentum excitations of the nucleon and delta states.

Introduction

The linear sigma model with quarks and chiral mesons has been used as an effective theory to describe the properties of light baryons, in particular the nucleon and the delta isobar. Usually, a variational method is considered, admitting the valence picture for the quarks and a mean-field inspired description for the meson clouds. Moreover, the hedgehog or some hedgehog like ansatz is assumed in most of the practical calculations[1-3].

The goal of this work is to explore another class of variational solutions. We shall consider an ansatz which is axial symmetric in both configuration and isospin spaces, i.e. an ansatz which is an eigenstate of the third components of angular momentum and isospin operators. A simplified version of the ansatz we are going to use was proposed in a seminal work by Providência and Urbano[4] and used subsequently in the framework of the cloudy-bag model[5] (see, for instance, Refs. [6-8]). However, the most relevant point in Ref. [4] was the proposal of the Peierls-Yoccoz projection method[9] from coherent states in the field of hadron physics, in order to construct model states with the proper symmetries which might be identified with physical states.

An axial ansatz can in principle be used as a starting point to describe angular momentum excitations of the nucleon and the delta. We remind that such states can not be described in a straightforward way from the hedgehog, since this state only contains components with angular momentum quantum number J *equal* to the isospin quantum number T. Therefore the only accessible states are the nucleon and the delta and not their angular momentum excitations for which $T \neq J$.

The usefulness of the hedgehog ansatz has been pointed out in several works: on the mathematical side, it simplifies considerably the formalism, and, on the physical side, it minimizes the energy of a quark-meson system, at least in the mean field approximation[10,11]. Even beyond the simple mean-field description the hedgehog has proven very successful[12]. We shall compare the results obtained from the axial ansatz with those obtained from the hedgehog in the mean field approximation. In a second step we shall apply the axial ansatz to describe baryons namely the ground state and angular momentum excitations in the isospin $T = 1/2$ (nucleon) and $T = 3/2$ (delta) channels.

Such program is carried out in the framework of the linear sigma model. Basically this is nothing but the implementation of the elegant ideas of Ref. [4] to a more realistic model. Providência and Urbano used a simple model with non-self-interacting pions coupled to a source (containing just bare nucleon) with a very schematic shape. The sigma model is a more sophisticated model which provides a good description of the nucleon and has a much stronger predictive power since it contains basically only one adjustable parame-

ter. The paper is organized as follows. First we present the basic features of the model (Section II). The axial ansatz and the mean field results are then presented and compared with the hedgehog (Section III). By means of the Peierls-Yoccoz projection method, which is briefly reviewed, positive parity states with good angular momentum and isospin quantum numbers are constructed (Section IV). The energies of such states are discussed and compared with data (Section V). Finally, conclusions are presented (Section VI).

II. The model

The linear sigma model with quarks is a $SU(2) \times SU(2)$ chiral invariant model. The chiral symmetry is spontaneously broken to $SU(2)$ and this is one of the most important features in the low energy domain which is well known from QCD. The spontaneous symmetry breaking shows up in the occurrence of non-vanishing vacuum expectation values for the chiral meson fields. We shall have $\langle 0|\vec{\pi}\rangle = 0$ and $\langle 0|\sigma_0|0\rangle = -f_\pi$, $|0>= 0$ where $\vec{\pi}$ and σ_0 are the pion (pseudoscalar-isovector) and the sigma (scalar-isoscalar) field operators and f_π is the pion decay constant. One usually introduces a new field, σ, whose vacuum expectation value is zero and therefore is related to σ_0 through $\sigma = \sigma_0 + f_\pi$.

The Lagrangian density of the model reads as [1]

$$\mathcal{L} = i\bar{q}\gamma^\mu\partial_\mu q + g\bar{q}(\sigma_0 + i\gamma_5\vec{\tau}\cdot\vec{\pi})q + \frac{1}{2}(\partial_\mu\sigma_0)^2\frac{1}{2}(\partial_\mu\vec{\pi})^2 - \mathcal{U}(\sigma_0,\vec{\pi}) \tag{1}$$

where g is the quark-meson coupling constant and $\mathcal{U}(\sigma_0,\vec{\pi})$ is the potential for the meson self-interactions (tilted mexican-hat) which is the responsible for the spontaneous chiral symmetry breaking. From (l) one obtains the Hamiltonian which can be cast in the form

$$H = H_q + H_{qM} + H_{q\sigma} + H_{q\pi} + H_\sigma + H_\pi + H_{n.l.} \ , \tag{2}$$

whose terms are:

$$H_q = \int d\mathbf{r}\bar{q}(\mathbf{r})i\gamma\cdot\nabla q(\mathbf{r}) \ , \tag{3}$$

the kinetic energy of the quarks;

$$H_{qM} = \int d\mathbf{r}gf_\pi\bar{q}(\mathbf{r})q(\mathbf{r}) \ , \tag{4}$$

the dynamical mass of the quarks;

$$H_{q\sigma} = -\int d\mathbf{r}g\sigma(\mathbf{r})\bar{q}(\mathbf{r})q(\mathbf{r}) \ , \tag{5}$$

the sigma-quark interaction Hamiltonian;

$$H_{q\sigma} = -\int d\mathbf{r}ig\bar{q}(\mathbf{r})\gamma_5\vec{\tau}\cdot\vec{\pi}(\mathbf{r})q(\mathbf{r}) \ , \tag{6}$$

the pion-quark interaction Hamiltonian;

$$H_\sigma = \int d\mathbf{r}\frac{1}{2}[P_\sigma^2(\mathbf{r}) + \nabla\sigma(\mathbf{r})\cdot\nabla\sigma(\mathbf{r}) + m_\sigma^2\sigma^2(\mathbf{r})], \tag{7}$$

the kinetic energy of the σ field (here P_σ is the conjugate momentum of the sigma field and m_σ its mass);

$$H_\pi = \int d\mathbf{r}\frac{1}{2}[\vec{P}_\pi(\mathbf{r})\cdot\vec{P}_\pi(\mathbf{r}) + \nabla\vec{\pi}(\mathbf{r})\cdot\nabla\vec{\pi}(\mathbf{r}) + m_\pi^2\vec{\pi}(\mathbf{r})\cdot\vec{\pi}(r)], \tag{8}$$

the kinetic energy of the pion field (here $\vec{P}_\pi$ is the conjugate momentum of the pion field and m_π the pion mass);

$$H_{n.l.} = \int d\mathbf{r}\frac{\lambda^2}{4}\{[\vec{\pi}(\mathbf{r})\cdot\vec{\pi}(\mathbf{r})]^2 + \sigma^4(\mathbf{r}) - 4\sigma^3(\mathbf{r})f_\pi + [2\sigma^2(\mathbf{r}) - 4f_\pi\sigma(\mathbf{r})]\vec{\pi}(\mathbf{r})\cdot\vec{\pi}(\mathbf{r})\} \ , \tag{9}$$

the meson-meson interaction energy (the symbol *n.l.* stands for *non-linear*). The parameter λ is related to the meson masses and to the pion decay constant:

$$\lambda^2 = \frac{m_\sigma^2 - m_\pi^2}{2f_\pi} \ . \tag{10}$$

In this paper we shall use the following parameter set: $m_\pi = 0.14\,\mathrm{GeV}$ and $f_\pi = 0.093\,\mathrm{GeV}$, which are fixed by experiment; for the sigma mass we take the most popular choice in non-topological soliton models, $m_\sigma = 1.2$ GeV, although for any value of the sigma mass above 0.9 GeV the results are essentially independent of the actual value of this parameter. Therefore, the coupling constant g is left as the only free parameter of the model.

III. The mean field approximation and the axial ansatz

The model defined by (1) is complex and one has to rely on some approximate scheme since the exact solutions are too difficult to be obtained. The main approach is to consider just valence quarks and to treat the mesonic degrees of freedom in the mean field approximation, i.e., to describe the meson clouds by coherent states. It is well known that such a treatment (considering a normal ordered Hamiltonian) is equivalent to the classical approximation which simply assumes that the meson field operators and conjugate momenta in the Hamiltonian (2) are c-functions.

The valence picture for the quarks does not mean that the polarization effects of the Dirac sea are not taken into account. In fact, in the valence picture, polarization effects are taken into account through the explicit consideration of dynamical chiral meson fields. Indeed it has been shown that for weak chiral fields in hedgehog the Nambu-Jona Lasinio model is equivalent to the linear sigma model if this is treated at the valence level only[13]. Thus, if one regards the Nambu-Jona Lasinio as a more fundamental model, to consider both Dirac sea states and dynamical meson fields in the sigma model corresponds to a kind of double-counting of the mesonic degrees of freedom. For the valence picture to hold there should be a reasonable gap between negative and positive energy states or, in other words, little interference between the valence and the sea quark orbitals.

III.1 Hedgehog

Before introducing the axial state which will be extensively used in this paper it is interesting to briefly mention the hedgehog since the axial and hedgehog results will be compared. In the hedgehog ansatz each quark occupies the same ls state, i.e. the same single particle quark state

$$\langle \mathbf{r}|q_h\rangle = \frac{1}{\sqrt{4\pi}} \begin{matrix} u(r) \\ i\sigma\cdot\hat{\mathbf{r}}v(r) \end{matrix} \quad |\chi_h\rangle \ . \tag{11}$$

The spin-isospin state $|\chi_h>$ is the same for the three quarks and is given in the non-strange sector by

$$|\chi_h\rangle = \frac{1}{\sqrt{2}}(|u\downarrow\rangle - |d\uparrow\rangle) \ . \tag{12}$$

The three quark state is therefore totally symmetric in the combined orbital-spin-isospin space and antisymmetry is imposed just in color space. Let us stress that the three quarks occupy the same orbital spin-isospin state in agreement with the spirit of the Hartree-Fock approximation for a many-body system.

The meson part of the baryon state is described by the coherent states $|\Pi_h\rangle$ and $|\Sigma_h\rangle$. One does not need to consider here the detailed structure of these states in the Fock space: it is enough to admit that the expectation values of the field operators in the hedgehog coherent states are

$$\langle\Pi_h|\pi_j(\mathbf{r})|\Pi_h\rangle = \hat{\mathbf{r}}_j\,\phi(r) \tag{13}$$

and

$$\langle\Sigma_h|\sigma(\mathbf{r})|\Sigma_h\rangle = \sigma(r). \tag{14}$$

The r.h.s. of these expressions can be viewed as the classical meson fields. It is important to notice the correlation between ordinary space and isospace expressed by (13) and the spherical symmetry of the mean (or classical) sigma field. Finally, we should stress that the baryon hedgehog state

$$|\psi_h\rangle = |q_h\,q_h\,q_h\rangle \otimes |\Pi_h\rangle \otimes |\Sigma_h\rangle \tag{15}$$

is an eigenstate of the grand-spin operator $\vec{\mathbf{G}} = \mathbf{J} + \vec{T}$ (sum of angular momentum and isospin operators) with eigenvalue zero.

III.2 Axial state

The axial state is clearly different from the hedgehog. The three quarks are still supposed to occupy the same lowest s state, i.e., they have in common the same radial functions $u(r)$ and $v(r)$, but now the *spin-isospin* state of the 3 quark cluster is not a simple product of three identical states as for the hedgehog. Instead it is given by

$$|A\rangle = \sum_{\alpha,\beta,\gamma} C_{\alpha\beta\gamma} |\chi_1\rangle_\alpha |\chi_2\rangle_\beta |\chi_3\rangle_\gamma \qquad (16)$$

where each of the single quark spin-isospin state is one of the basis states $u\uparrow$, $u\downarrow$, $d\uparrow$ and $d\downarrow$, and $C_{\alpha\beta\gamma}$ are appropriate coefficients such that, in the baryon space, the state (16) reads

$$|A\rangle = \cos\delta \ |N^+_{1/2}\rangle + \sin\delta | \ \Delta^+_{1/2}\rangle \ . \qquad (17)$$

The parameter δ is to be treated variationally, and it allows for different weights of bare nucleon or bare delta in the bare baryon state. We shall denote by $|(qqq)_A\rangle$ the three quark state, i.e. the state for which each quark occupies the same radial state, with the radial functions as in (11), and with the spin-isospin state given by (17). The three quark state $|(qqq)_A\rangle$ is not an eigenstate of the angular momentum or the isospin bare baryon operators but it is an eigenstate of their third components, i.e.

$$J^{(B)}_z |(qqq)_A\rangle = T^{(B)}_3 |(qqq)_A\rangle = \frac{1}{2} |(qqq)_A\rangle \ . \qquad (18)$$

As for the hedgehog the antisymmetry of the axial three quark state is only imposed in color space.

The quantum state describing the mesons should be consistent with the fact that quarks are in $j = \frac{1}{2}$ states and are isospin $t = \frac{1}{2}$ states. In the mean field approximation this implies that only s-wave quanta (for sigma) and p-wave quanta (for pion) are allowed (beyond the mean field, the interaction with the pions may induce single particle quark states with higher j but admixtures of these excited quark states are small and can be neglected). To describe the meson clouds we shall use coherent states, whose explicit form will be presented in Section IV. At this point it is enough to state that the axial coherent states $|\Pi_A\rangle$ and $|\Sigma_A\rangle$ yield the following expectation values of the field operators:

$$\langle \Pi_A | \pi_j(\mathbf{r}) | \Pi_A \rangle = \delta_{j3} \frac{z}{r} \phi(r) \qquad (19)$$

and

$$\langle \Sigma_A | \sigma(\mathbf{r}) | \Sigma_A \rangle = \sigma(r) \ . \qquad (20)$$

From these expressions one infers that both $|\Pi_A\rangle$ and $|\Sigma_A\rangle$ are eigenstates of the third components of the angular momentum and isospin meson operators with eigenvalue 0, i.e.

$$J^{(\pi)}_z |\Pi_A\rangle = T^{(\pi)}_3 |\Pi_A\rangle = 0 \qquad (21)$$

$$J^{(\sigma)}_z |\Sigma_A\rangle = T^{(\sigma)}_3 |\Sigma_A\rangle = 0 \ . \qquad (22)$$

The (normalized) axial baryon trial state is

$$|\psi_A\rangle = |(qqq)_A\rangle \otimes |\Pi_A\rangle \otimes |\Sigma_A\rangle \qquad (23)$$

and from (18), (21) and (22) one concludes that it is an eigenstate of the third components of the *total* angular momentum and isospin operators (bare baryon plus mesons) with eigenvalue 1/2:

$$J_z |\psi_A\rangle = T_3 |\psi_A\rangle = \frac{1}{2} |\psi_A\rangle \ . \qquad (24)$$

III.3 Mean field approximation

The mean field energy is the expectation value of the normal ordered Hamiltonian (2) in the state (23)

$$E_A = \langle \psi_A | : H : | \psi_A \rangle \ . \qquad (25)$$

A variational principle applied to this energy will be used to determine the best radial profiles $u(r)$, $v(r)$ for the quarks, $\sigma(r)$ for the sigma, $\phi(r)$ for the pion, and the bare nucleon - bare delta mixing angle, δ, in (17).

Evaluation of (25) yields

$$E_A = 4\pi \int_0^\infty r^2 dr \left\{ \frac{3}{4\pi}\left[u\frac{dv}{dr} - v\frac{du}{dr} + 2\frac{uv}{r} + gf_\pi(u^2-v^2) - g\sigma(u^2-v^2) + \frac{2}{9}guv\phi A(\delta)\right]\right.$$
$$\left. + \frac{1}{2}\left[\left(\frac{d\sigma}{dr}\right)^2 + m_\sigma^2\sigma^2\right] + \frac{1}{6}\left[\left(\frac{d\phi}{dr}\right)^2 + 2\frac{\phi^2}{r^2} + m_\pi^2\phi^2\right] + \frac{\lambda^2}{4}\left[\frac{\phi^4}{5} + \sigma^4 - 4f_\pi\sigma^3 + \frac{2}{3}\phi^2(\sigma^2 - 2f_\pi\sigma)\right]\right\} . \quad (26)$$

In this expression,

$$A(\delta) = \langle A| \sum_{a=1}^{3} \sigma_z^{(a)} \tau_3^{(a)} |A\rangle \quad (27)$$

($\sigma_i^{(a)}$ and $\tau_j^{(a)}$ with $i = x, y, z$ and $j = 1, 2, 3$ are the Pauli matrices for the quark a in spin and isospin spaces, respectively). It turns out to be more convenient to work in the spin-isospin bare baryon space rather than in the quark space. To this end we replace the quark operator in (27) by the corresponding baryon operator[14]

$$b_{ij} = \sum_{a=1}^{3} \sigma_i^{(a)} \tau_j^{(a)} = \frac{5}{3} B_{ij}, \quad (28)$$

where

$$B_{ij} = \sigma_i^{NN}\tau_i^{NN} + \sqrt{\frac{72}{25}}(\sigma_i^{N\Delta}\tau_j^{N\Delta} + \sigma_i^{\Delta N}\tau_j^{\Delta N}) + \frac{4}{5}\sigma_i^{\Delta\Delta}\tau_j^{\Delta\Delta} \quad (29)$$

acts now in the bare baryon space. We use $\sigma_i^{BB'}$ and $\tau_j^{BB'}$ to denote the transition matrices between bare baryon states B' and B in the spin and isospin spaces respectively (for instance, σ^{NN} and τ^{NN} are the Pauli matrices in the bare nucleon space, acting in spin and isospin respectively). The explicit form of these matrices may be found in the Appendix A of Ref. [7] and, for the quantity (27), one finds

$$A(\delta) = \frac{5}{3}\cos^2\delta + \frac{8\sqrt{2}}{3}\sin\delta\cos\delta + \frac{1}{3}\sin^2\delta \ . \quad (30)$$

The variational method consists in minimizing the energy functional (26) with respect to the radial profiles and to the mixing angle δ. However, the variations must be constrained by requiring the norm of the quark spinor,

$$N = \int_0^\infty r^2 dr (u^2 + v^2), \quad (31)$$

to be equal to 1. This requirement is implemented in the variational principle by means of a Lagrange multiplier ϵ. Accordingly, we demand that the functional $F[\Omega_i] = E_A - 3\epsilon N$ (with $\Omega_i = u, v, \sigma, \phi$) satisfies the condition $\delta F/\delta\Omega_i = 0$, from which we obtain the following set of differential equations:

$$\frac{du}{dr} = [g(\sigma - f_\pi) - \epsilon]v + \frac{g}{9}A(\delta)\phi u \tag{32}$$

$$\frac{dv}{dr} = -\frac{2v}{r} + [g(\sigma - f_\pi) + \epsilon]u - \frac{g}{9}A(\delta)\phi v \tag{33}$$

$$\frac{d^2\sigma}{dr^2} = -\frac{2}{r}\frac{d\sigma}{dr} + m_\sigma^2\sigma - \frac{3}{4\pi}g(u^2 - v^2) + \lambda^2\left[\sigma^3 - 3f_\pi\sigma^2 + \frac{1}{3}(\sigma - f_\pi)\phi^2\right] \tag{34}$$

$$\frac{d^2\phi}{dr^2} = -\frac{2}{r}\frac{d\phi}{dr} + \frac{2}{r^2}\phi + m_\pi^2\phi + \frac{g}{2\pi}A(\delta)uv + \lambda^2\left[\frac{3}{5}\phi^3 + \phi(\sigma^2 - 2f_\pi\sigma)\right] \ . \tag{35}$$

These equations are supplemented by the following boundary conditions: at $r = 0$,

$$v = 0, \quad \phi = 0, \quad \frac{d\sigma}{dr} = 0, \tag{36}$$

which guarantee that the differential equations above are non-divergent at the origin; at large r (in practice $r = r_{\max} \simeq 10$ fm) the boundary conditions are

$$r\frac{d\sigma}{dr} + (1 + rm_\sigma)\sigma = 0 \tag{37}$$

$$r(1 + m_\pi r)\frac{d\phi}{dr} + (2 + m_\pi r + r^2 m_\pi^2)\phi = 0 \tag{38}$$

$$\left[r\sqrt{gf_\pi - \epsilon} + \frac{1}{\sqrt{gf_\pi + \epsilon}}\right]u - r\sqrt{gf_\pi + \epsilon}v = 0. \tag{39}$$

The functions $u(r)$ and $\sigma(r)$ behave asymptotically as $\ell = 0$ Yukawa wave functions while $v(r)$ and $\phi(r)$ as $\ell = 1$ Yukawa wave functions. Notice that the asymptotic quarks have masses $\sqrt{(gf_\pi)^2 - \epsilon^2}$. This means that the Lagrange multiplier ϵ, whose physical meaning is of a quark eigenenergy, lies in the range $-gf_\pi \leq \epsilon \leq gf_\pi$.

For a given δ, the set of differential equations (32-35) is solved numerically. One of the most stringent tests of the numerical procedure is the comparison of the energy E_A as given by (26), now computed with the solutions u, v, σ and ϕ of the differential equations, and the so-called Rafelski energy which is given by [15]

$$E_R = \int d\mathbf{r}\left[4U(\sigma,\phi) - (\sigma + f_\pi)\frac{dU}{d\sigma} - \sum_{j=1}^{3}\phi_j\frac{dU}{d\phi_j}\right] \ . \tag{40}$$

Typically we could obtain an agreement between E_A and E_R in, at least, seven significant digits.

III.4 Results

Normalized solutions of Eqs. (32-35) can be obtained only for $g > 5$. For smaller values of g the strength of the interaction is not enough to allow the soliton to be formed. However, only for $g > 5.5$ the soliton becomes stable in the sense that its energy is lower than the energy of three free quarks. This can be seen in Fig. 1. We should mention that irrespective of g, the minimal energy is always obtained for $\delta = 35.26°$, which corresponds to the maximum of the function (30). We shall always use this value for δ (namely in the figures presented in this section) unless stated otherwise.

For sufficiently large coupling constant, there are two types of solutions represented by the two branches in Fig. 1 joining at the cusp for $g \simeq 5$. The solutions lying in the upper branch are always unstable: their energies are larger than $3gf_\pi$, the energy (mass) of the three free constituent quarks (dashed straight line in Fig. 1). The lower branch is absolutely stable beyond the crossing with the dashed line. It is also interesting to look at the behavior of the quark eigenvalue ϵ as a function of g. This is shown in Fig. 2 (full curve) where the quark dynamical mass is also represented (dashed straight line). The upper part of the curve $\epsilon(g)$ corresponds to the unstable soliton whereas the lower one corresponds to the stable soliton. In Figs. 3 and 4 the quark and the meson radial profiles are shown in dependence of r for $g = 5.6$. The dashed curves correspond to the unstable solutions and the solid curves to the stable ones. For the unstable solutions the chiral fields are

weak (the σ function never crosses zero), the soliton is large (see quark radial functions $u(r)$ and $v(r)$) and the lower component in the quark spinor is much smaller than the upper component. The stable soliton is characterized by a much smaller size, larger $u(r)$ and $v(r)$ components at small and intermediate distances and relatively strong pion and sigma radial fields. These behaviors are qualitatively similar to those found for the hedgehog soliton[3].

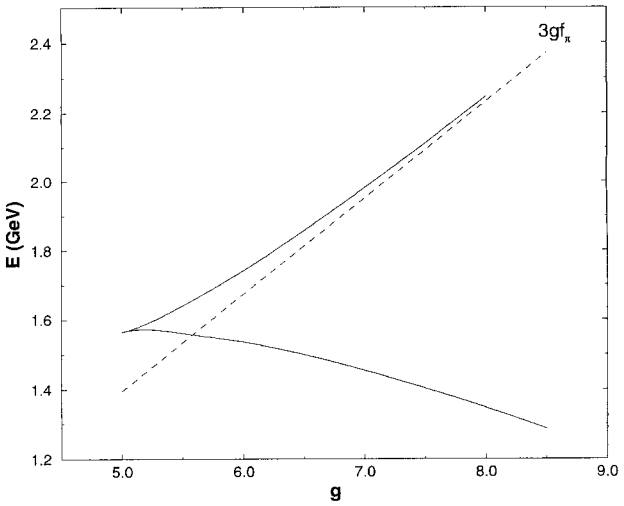

Figure 1: Energy of the axial soliton (solid curves) in dependence of g. The upper and the lower branches correspond to the unstable and to the stable solitons, respectively. The dashed line represents the dynamical mass of three quarks.

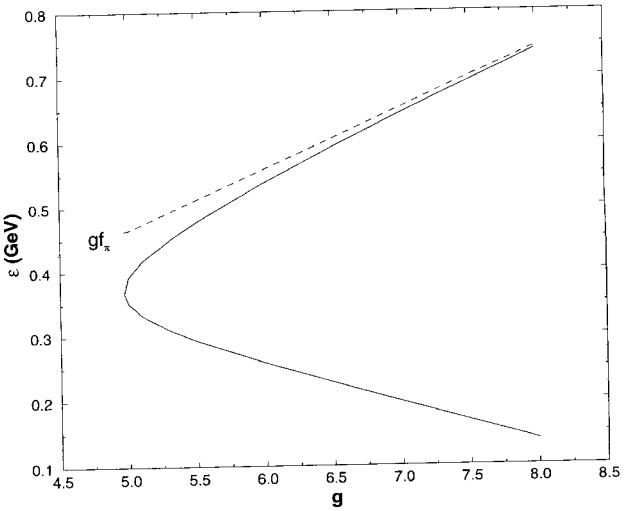

Figure 2. Quark eigenvalue in dependence of g. The upper and the lower parts of the curve correspond to the unstable and to the stable solitons, respectively. The dashed line represents the dynamical mass of a quark.

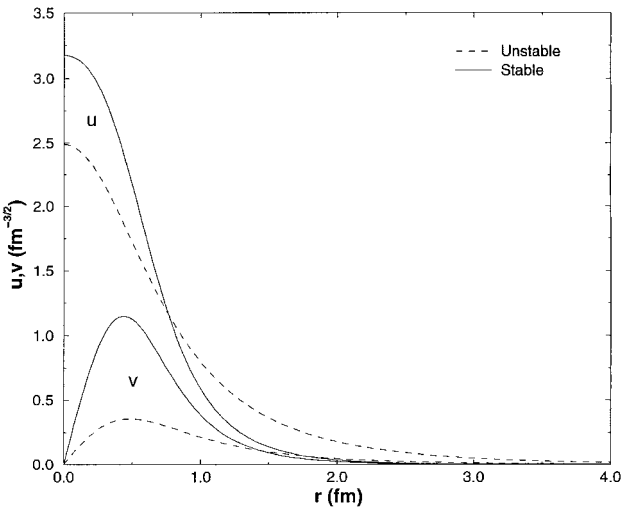

Figure 3. Quark radial functions, $u(r)$ and $v(r)$, for the stable and the unstable solitons, using $g = 5.6$.

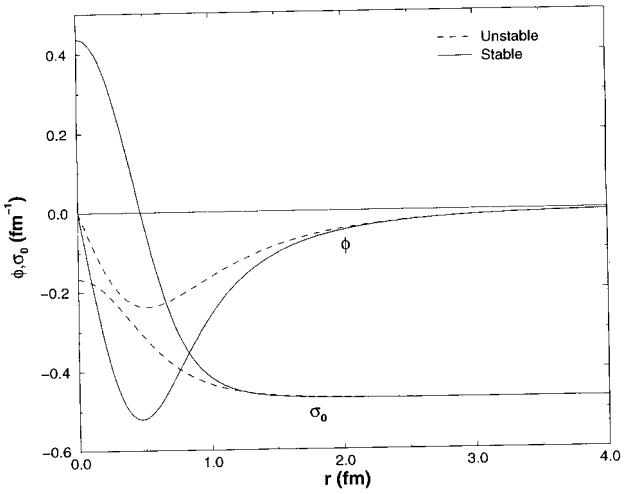

Figure 4. Meson radial profiles $\sigma(r)$ and $\phi(r)$, for the stable and the unstable solitons, using $g = 5.6$

It is instructive to compare the axial results with the hedgehog ones. The energy of both states, in the mean field approximation, is plotted against g in Fig. 5. Only the curves corresponding to the stable solitons are shown. The hedgehog energy curve lies always bellow the axial one and decreases very rapidly. In Fig. 6 it is shown the eigenvalue as function of g and the trend is similar. In the axial case the eigenvalue is well above zero, thus justifying the valence picture. For the hedgehog, when $g > 5.5$ the eigenvalue becomes negative and the total energy becomes too close the nucleon energy.

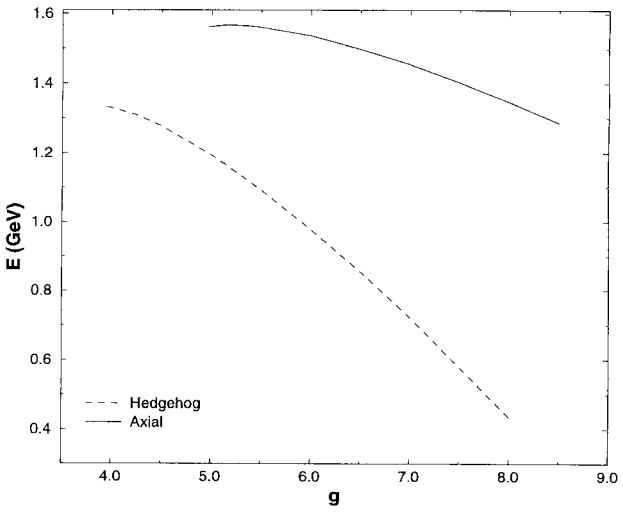

Figure 5. For the stable solitons, plotted are the axial and the hedgehog energies in dependence of the coupling constant of the model.

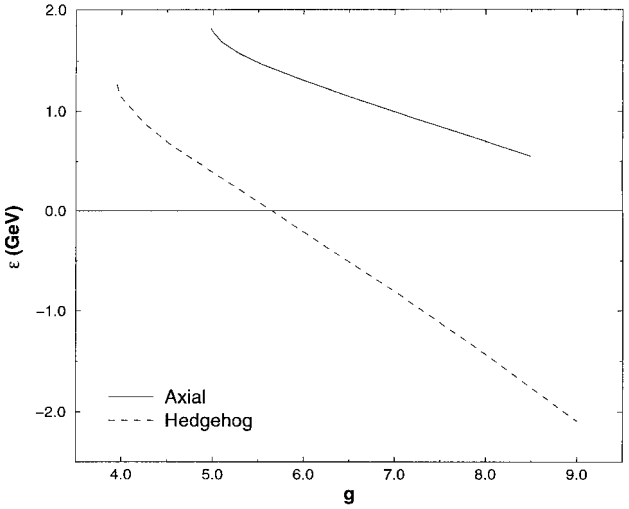

Figure 6. For the stable solitons, plotted are the quark eigenenergies for the axial and the hedgehog solitons.

Regarding the radial functions, and using the same coupling constant, the upper component of the quark spinor is bigger near the origin in the case of the hedgehog and the soliton is smaller. Accordingly, the binding fields $\phi(r)$ and $\sigma(r)$ are stronger for the hedge-hog at small and intermediate distances. Asymptotically these fields behave similarly in the axial and the hedgehog cases.

IV. Projection from the axial state

The axial state introduced in the previous section is not an eigenstate of J^2 or T^2 (although it is an eigenstate of J_z and T_3) and therefore cannot directly describe physical baryon states.

However, the Peierls-Yoccoz operator[16]

$$P^J_{MK} = \frac{2J+1}{8\pi^2}\int d\Omega \mathcal{D}^{J*}_{MK}(\Omega)R(\Omega), \qquad (41)$$

where $\Omega \equiv (\alpha, \beta, \gamma)$ is the set of Euler angles, $\mathcal{D}^J_{MK}(\Omega)$ is the Wigner function and $R(\Omega)$ is the rotation operator, can be used to extract states with good angular momentum J from a state $|\psi\rangle$, like the axial state (23) or the hedgehog state (15). To construct isospin eigenstates, a similar operator can be considered acting on isospin space

$$P^T_{M_T K_T} = \frac{2T+1}{8\pi^2}\int d\Omega_T \mathcal{D}^{T*}_{MK}(\Omega_T)R(\Omega_T), \qquad (42)$$

with an obvious notation for quantities in isospace. The operator (41) may alternatively be expressed as $P^J_{MK} = |JM\rangle\langle JK|$ (notice that only if $M = K$ the operator becomes a projector). Therefore, the effect of its operation on an angular momentum eigenstate $|J'M'\rangle$ is

$$P^J_{MK}|J'M'\rangle = |JM\rangle\delta_{JJ'}\delta_{KM'}\ , \qquad (43)$$

and similarly for the operator (42) acting on isospin eigenstates. The following properties, $P^J_{MK}P^{J'}_{M'K'} = P^J_{MK'}\delta_{JJ'}\delta_{KM'}$ and $(P^J_{MK})^\dagger = P^J_{MK}$ are also very useful.

The symmetries of the hedgehag considerably simplify the combined angular momentum - isospin projection. In fact, only one projection, either in angular momentum or in isospin, is needed, since, as mentioned before, only $J = T$ states are present in the hedgehog. A simplification in the formalism also occurs if the 'unprojected state', $|\psi\rangle$, is axially symmetric.

Let us denote a state with angular momentum quantum numbers (J, M) and isospin quantum numbers (T, M_T) by $|JTMM_T\rangle$. Here we are not much interested on how these states (projected states) can be obtained from $|\psi\rangle$ by means of the operators (41) and (42), but rather on the evaluation of expectation values of certain operators in such states. For instance, the energy of the state $|JTMM_T\rangle$ is the following expectation value of the normal ordered Hamiltonian:

$$E^{JT} = \langle JTMM_T| :\ H\ : |JTMM_T\rangle\ . \qquad (44)$$

This energy is independent of M and M_T since the Hamiltonian is a scalar-isoscalar operator, and it is given by [4, 7, 8]

$$E^{JT} = \frac{h^{JT}_{\frac{1}{2}\frac{1}{2}}}{n^{JT}_{\frac{1}{2}\frac{1}{2}}} = \frac{\langle\psi_A| \ : \ H \ : \ P^J_{\frac{1}{2}\frac{1}{2}} P^T_{\frac{1}{2}\frac{1}{2}}|\psi_A\rangle}{\langle\psi_A|P^J_{\frac{1}{2}\frac{1}{2}} P^T_{\frac{1}{2}\frac{1}{2}}|\psi_A\rangle} \ . \qquad (45)$$

The denominator in (45)

$$P^{JT} = n^{JT}_{\frac{1}{2}\frac{1}{2}} = \langle\psi_A|P^J_{\frac{1}{2}\frac{1}{2}} P^T_{\frac{1}{2}\frac{1}{2}}|\psi_A\rangle \ , \qquad (46)$$

which looks like a normalization factor, is nothing but the probability of finding the state $|JT\frac{1}{2}\frac{1}{2}\rangle = P^J{}_{\frac{1}{2}\frac{1}{2}} P^T_{\frac{1}{2}\frac{1}{2}}|\psi_A\rangle$ in the "intrinsic" state $|\psi_A\rangle$. (Notice that $P^J_{\frac{1}{2}\frac{1}{2}}$ and $P^T_{\frac{1}{2}\frac{1}{2}}$ are projectors.)

The task now is to determine the energy and the norm "kernels", $h^{JT}_{\frac{1}{2}\frac{1}{2}}$ and $n^{JT}_{\frac{1}{2}\frac{1}{2}}$, respectively, and this is the program for the next two sub-sections.

IV.1 Norm kernel

Let us first compute $n^{JT}_{\frac{1}{2}\frac{1}{2}}$, whose explicit expression is (see (46) and (41,42))

$$n^{JT}_{\frac{1}{2}\frac{1}{2}} = \frac{2J+1}{8\pi^2}\frac{2T+1}{8\pi^2}\int d\Omega d\Omega_T \mathcal{D}^{J^*}_{\frac{1}{2}\frac{1}{2}}(\Omega)\mathcal{D}^{T^*}_{\frac{1}{2}\frac{1}{2}}(\Omega_T)\langle\psi_A|R(\Omega)R(\Omega_T)|\psi_A\rangle \ . \qquad (47)$$

Making use of the axial symmetry (24) of the state $|\psi_A\rangle$ and remembering that $R(\Omega) = R(\alpha)R(\beta)R(\gamma) = e^{-i\alpha J_z}e^{-i\beta J_y}e^{-i\gamma J_z}$ and that the Wigner function $\mathcal{D}^{J^*}_{\frac{1}{2}\frac{1}{2}} = d^J_{\frac{1}{2}\frac{1}{2}}(\beta)e^{i(\alpha+\gamma)/2}$ (similar expressions hold for isospin), expression (47) reduces to

$$n^{JT}_{\frac{1}{2}\frac{1}{2}} = \frac{2J+1}{2}\frac{2T+1}{2}\int_0^\pi \sin\beta d\beta \int_0^\pi \sin\beta_T d\beta_T d^J_{\frac{1}{2}\frac{1}{2}}(\beta)d^T_{\frac{1}{2}\frac{1}{2}}(\beta_T)n_B(\beta,\beta_T)n_\sigma(\beta,\beta_T)n_\pi(\beta,\beta_T) \qquad (48)$$

where

$$n_B(\beta,\beta_T) = \langle(qqq)_A|R_B(\beta)R_B(\beta_T)|(qqq)_A\rangle \qquad (49)$$

$$n_\sigma(\beta,\beta_T) = \langle\Sigma_A|R_\sigma(\beta)R_\sigma(\beta_T)|\Sigma_A\rangle \qquad (50)$$

$$n_\pi(\beta,\beta_T) = \langle\Pi_A|R_\pi(\beta)R_\pi(\beta_T)|\Pi_A\rangle \ . \qquad (51)$$

In these expressions we have considered explicitly the rotation and iso-rotation operators for the bare baryon, the sigmas and the pions, using a self-explanatory notation.

The sigma meson quanta are s-waves and the sigma is an intrinsic scalar-isoscalar. Therefore, the coherent state of sigmas $|\Sigma_A\rangle$ is not affected by the (iso)rotation and hence

$$n_\sigma(\beta,\beta_T) = 1. \qquad (52)$$

Regarding the norm overlap for the bare baryon state–expression (49)–the orbital part of the quarks do not contribute since it is kept invariant under (iso)rotations, and therefore

$$n_B(\beta,\beta_T) = \langle A|R(\beta)R(\beta_T)|A\rangle \qquad (53)$$

which is readily evaluated yielding

$$N_B(\beta,\beta_T) = \cos^2\ \delta d^{\frac{1}{2}}_{\frac{1}{2}\frac{1}{2}}(\beta)d^{\frac{1}{2}}_{\frac{1}{2}\frac{1}{2}}(\beta_T) + \sin^2\ \delta d^{\frac{3}{2}}_{\frac{1}{2}\frac{1}{2}}(\beta)d^{\frac{3}{2}}_{\frac{1}{2}\frac{1}{2}}(\beta_T). \qquad (54)$$

In order to compute the pion contribution to the norm overlap–expression (51)–let us first write down the coherent state describing the pions:

$$|\Pi_A\rangle = \mathcal{N}[\xi] e^{\sum_{j=1}^{3} \int d\mathbf{k} \xi_j(\mathbf{k}) a_j^\dagger(\mathbf{k})} |0\rangle, \qquad (55)$$

where $a_j^\dagger(\mathbf{k})$ is the creation operator for a plane wave pion with momentum $\mathbf{k}$ and isospin (cartesian) index $j, \xi_j(\mathbf{k})$ is the amplitude of the coherent state and $\mathcal{N}[\xi]$ is just a normalization factor.

The pion field operator expansion in plane wave modes reads as

$$\pi_j(\mathbf{r}) = \frac{1}{(2\pi)^{3/2}} \int \frac{d\kappa}{\sqrt{2\omega_k}} \langle [a_j^\dagger(\mathbf{k}) e^{-i\mathbf{k}\cdot\mathbf{r}} + a_j(\mathbf{k}) e^{i\mathbf{k}\cdot\mathbf{r}}\rangle] \qquad (56)$$

where $\omega_k = \sqrt{k^2 + m_\pi^2}$. Taking the expectation value of this operator in the coherent state (55) and using essentially the property

$$a_j(\mathbf{k})|\Pi_A\rangle = \xi_j(\mathbf{k})|\Pi_A\rangle \qquad (57)$$

one finds that the amplitude in (55) compatible with Eq. (19) is given by

$$\xi_j(\mathbf{k}) = -i\delta_{j3} \frac{k_z}{k} \varphi(k) \qquad (58)$$

where the function $\varphi(k)$ and the function $\phi(r)$ (Eq. (19)) are related by

$$\xi(\mathbf{k}) = \sqrt{\frac{2}{\omega_k}} \varphi(k) = \sqrt{\frac{2}{\pi}} \int_0^\infty r^2 dr j_1(kr) \phi(r). \qquad (59)$$

The number of pions in the coherent state (55) is a theoretical concept of great significance in the projection formalism, as we shall see. Such quantity is just the expectation of the number operator in the coherent state (55):

$$N_\pi = \langle \Pi_A | n | \Pi_A \rangle = \langle \Pi_A | \sum_{j=1}^{3} \int d\mathbf{k} a_j^\dagger(\mathbf{k}) a_j(\mathbf{k}) | \Pi_A \rangle. \qquad (60)$$

Using the property (57) and the explicit form of the amplitude (58) the evaluation of N_π is straightforward yielding

$$\begin{aligned} N_\pi &= \sum_{j=1}^{3} \int d\mathbf{k} \xi_j^*(\mathbf{k}) \xi_j(\mathbf{k}) = \frac{4\pi}{3} \int_0^\infty k^2 dk \varphi^2(k) \\ &= \frac{4}{3} \int_0^\infty k^2 dk \omega_k \int_0^\infty r^2 dr j_1(kr) \phi(r) \int_0^\infty r'^2 dr' j_1(kr') \phi(r'). \end{aligned} \qquad (61)$$

The normalization factor in (55) is given in terms of this quantity:

$$\mathcal{N} = e^{-N_\pi/2}. \qquad (62)$$

The rotated and isorotated axial coherent state (55) is again a coherent state but with new amplitudes $\xi_j'(\mathbf{k})$:

$$R_\pi(\beta) R_\pi(\beta_T) |\Pi_A\rangle = \mathcal{N}[\xi] e^{\sum_{j=1}^{3} \int d\mathbf{k} \xi_j'(\mathbf{k}) a_j^\dagger(\mathbf{k})} |0\rangle. \qquad (63)$$

These new amplitudes are related to the old ones through

$$\xi_j'(\mathbf{k}) = \sum_{j'=1}^{3} \mathcal{R}_{jj'}(\beta_T) \xi_j'(\mathcal{R}^{-1}(\beta)\mathbf{k}), \qquad (64)$$

where $\mathcal{R}$ is the standard 3 x 3 (iso)rotation matrix; using (58), $\xi_j'(\mathbf{k})$ is obtained explicitly. The overlap (51) between the rotated and the unrotated coherent states can now be computed, yielding

$$n_\pi(\beta, \beta_T) = \mathcal{N}^2[\xi] e^{N_\pi \cos\beta \cos\beta_T}. \qquad (65)$$

Finally, from (48-51) on one hand, and from (52,54,65) on the other hand, the norm kernel

$$n^{JT}_{\frac{1}{2}\frac{1}{2}} = e^{-N_\pi} \frac{2J+1}{8\pi^2} \frac{2T+1}{8\pi^2} F^{JT}, \qquad (66)$$

where

$$F^{JT} = \cos^2\delta f_N^{JT} + \sin^2\delta f_\Delta^{JT} \ . \qquad (67)$$

The functions f_N^{JT} and f_Δ^{JT} are given by

$$f_N^{JT} = \int_0^\pi \sin\beta d\beta \int_0^\pi \sin\beta_T d\beta_T d^J_{\frac{1}{2}\frac{1}{2}}(\beta) d^T_{\frac{1}{2}\frac{1}{2}}(\beta_T) d^{\frac{1}{2}}_{\frac{1}{2}\frac{1}{2}}(\beta) d^{\frac{1}{2}}_{\frac{1}{2}\frac{1}{2}}(\beta_T) e^{N_\pi \cos\beta\cos\beta_T} \ . \qquad (68)$$

and

$$f_\Delta^{JT} = \int_0^\pi \sin\beta d\beta \int_0^\pi \sin\beta_T d\beta_T d^J_{\frac{1}{2}\frac{1}{2}}(\beta) d^T_{\frac{1}{2}\frac{1}{2}}(\beta_T) d^{\frac{3}{2}}_{\frac{1}{2}\frac{1}{2}}(\beta) d^{\frac{3}{2}}_{\frac{1}{2}\frac{1}{2}}(\beta_T) e^{N_\pi \cos\beta\cos\beta_T} \ . \qquad (69)$$

These integrals can be evaluated analytically. However, the final expressions are lengthy, and the most practical way to compute them is to expand the exponential in power series and perform a termwise integration[8]. As an example of the procedure let us consider $J = T = \frac{1}{2}$ in (68) (it is more convenient to change to new variables $x = \cos\theta$ and $y = \cos\theta_T$)

$$f_N^{\frac{1}{2}\frac{1}{2}} = \int_{-1}^1 dx \int_{-1}^1 dy \frac{x+1}{2}\frac{y+1}{2} e^{N_\pi xy} = \frac{1}{4}\sum_{n=0}^\infty \frac{N_\pi^n}{n!}\left(\frac{1-(-1)^{n+2}}{n+2} + \frac{1-(-1)^{n+1}}{n+1}\right)^2 . \qquad (70)$$

This series is rapidly convergent for typical values of $N_\pi (0 < N_\pi \leq 1.5)$. For high J and T values this method has proven to be very efficient.

IV.2 Energy kernel

Let us turn now to the evaluation of the numerator of (45). Using the decomposition (2) of the Hamiltonian the energy kernel can be written as

$$\begin{aligned} h^{JT}_{\frac{1}{2}\frac{1}{2}} &= \langle\psi_A| : H_q + H_{qM} + H_{q\sigma} + H_{q\pi} + H_\pi + H_\sigma + H_{n.l.} : |\psi_A\rangle \\ &= h_o^{JT} + h_\pi^{JT} + h_{q\pi}^{JT} + H_{n.l.}^{JT} \ , \end{aligned} \qquad (71)$$

where the first term corresponds to the parts (3-5,7) of the Hamiltonian and the other three terms, to (8), (6) and (9), respectively. The quantity h_o^{JT} includes those terms which are not affected by the projection (the quark kinetic energy, the quark dynamical mass, the quark-sigma interaction energy and the sigma kinetic energy) and reads

$$h_o^{JT} = n^{JT}_{\frac{1}{2}\frac{1}{2}} E_o \qquad (72)$$

where (see Eq. (26))

$$E_o = \int_0^\infty r^2 dr \left\{ 3\left[u\frac{dv}{dr} - v\frac{du}{dr} + 2\frac{uv}{r} + g f_\pi(u^2 - v^2) - g\sigma(u^2 - v^2)\right] + 2\pi\left[\left(\frac{d\sigma}{dr}\right)^2 + m_\sigma^2\sigma^2\right]\right\} \qquad (73)$$

is the classical or the mean field energy for the quarks (including kinetic and mass energy), the sigmas and the quark-sigma interaction.

In order to compute

$$h_\pi^{JT} = \langle\psi_A| \ : \ H_\pi \ : P^J_{\frac{1}{2}\frac{1}{2}} P^T_{\frac{1}{2}\frac{1}{2}} |\psi_A\rangle, \tag{74}$$

the second term in (71), it is better to consider the kinetic pion Hamiltonian operator (8) in the alternative form

$$H_\pi = \sum_{j=1}^{3} \int d\mathbf{k}\omega_k a_j^\dagger(\mathbf{k}) a_j(\mathbf{k}), \tag{75}$$

since the property (57) of the coherent states may be then directly applied. The result is

$$h_\pi^{JT} = e^{-N_\pi} \frac{2J+1}{2} \frac{2T+1}{2} E_\pi G^{JT} \ , \tag{76}$$

where (see Eq. (26))

$$E_\pi = \frac{2\pi}{3} \int_0^\infty r^2 dr \left[\left(\frac{d\phi}{dr} \right)^2 + 2\frac{\phi^2}{r^2} + m_\pi^2 \phi^2 \right] \tag{77}$$

is the classical (or mean field) kinetic energy of the pions and

$$G^{JT} = \cos^2\delta \ g_N^{JT} + \sin^2\delta \ g_\Delta^{JT} \tag{78}$$

is a projection coefficient. This is given in terms of the following functions:

$$g_N^{JT} = \int_0^\pi d\beta \sin\beta \ \int_0^\pi d\beta \ \sin\beta_T d^J_{\frac{1}{2}\frac{1}{2}}(\beta) d^T_{\frac{1}{2}\frac{1}{2}}(\beta_T) e^{N_\pi \cos\beta\cos\beta_T} d^{\frac{1}{2}}_{\frac{1}{2}\frac{1}{2}}(\beta) d^{\frac{1}{2}}_{\frac{1}{2}\frac{1}{2}}(\beta_T) \cos\beta\cos\beta_T \ . \tag{79}$$

and

$$g_\Delta^{JT} = \int_0^\pi d\beta \sin\beta \int_0^\pi d\beta \sin \ \beta_T d^J_{\frac{1}{2}\frac{1}{2}}(\beta) d^T_{\frac{1}{2}\frac{1}{2}}(\beta_T) e^{N_\pi \cos\beta\cos\beta_T} d^{\frac{3}{2}}_{\frac{1}{2}\frac{1}{2}}(\beta) d^{\frac{3}{2}}_{\frac{1}{2}\frac{1}{2}}(\beta_T) \cos\beta\cos\beta_T \ . \tag{80}$$

Again, the best way to compute (79,80) is to expand the exponential and integrate term by term, as explained at the end of the previous sub-section.

The evaluation of the quark-pion interaction term–the third term in (71)–which is given by

$$h_{q\pi}^{JT} = \langle\psi_A| \ : \ H_{q\pi} \ : P^J_{\frac{1}{2}\frac{1}{2}} P^T_{\frac{1}{2}\frac{1}{2}} |\psi_A\rangle, \tag{81}$$

is easier if one uses the pion field expansion (56) in the expression (6) of $H_{q\pi}$. One gets

$$h_{q\pi}^{JT} = e^{-N_\pi} \frac{2J+1}{2} \frac{2T+1}{2} E_{q\pi} T^{JT} \ , \tag{82}$$

where

$$E_{q\pi} = \frac{2}{3} g \int_0^\infty r^2 dr \ u \ v \ \phi \tag{83}$$

and the projection coefficient T^{JT} is given in terms of the functions defined by (68,69):

$$T^{JT} = \frac{5}{3}\cos^2\delta f_N^{JT} + \frac{4\sqrt{2}}{3}\sin\delta\cos\delta(f_N^{JT} + f_\Delta^{JT}) + \frac{1}{3}\sin^2\delta f_\Delta^{JT} \ . \tag{84}$$

Finally one has to compute the non-linear part of the Hamiltonian, Eq. (9). In (9), those terms which do not involve the pion field are not changed with respect to the mean-field result but this is not the case for the quartic and the quadratic terms in the pion field. The last term in (71) may be decomposed as

$$h_{n.l.}^{JT} = \langle\psi_A| \ : \ H_{n.l.} \ : P^J_{\frac{1}{2}\frac{1}{2}} P^T_{\frac{1}{2}\frac{1}{2}} |\psi_A\rangle = h_{n.l.(o)}^{JT} + h_{n.l.(\pi^2)}^{JT} + h_{n.l.(\pi^4)}^{JT}. \tag{85}$$

The term unaffected by the projection has a structure similar to (72) i.e.

$$h_{n.l.(o)}^{JT} = n_{\frac{1}{2}\frac{1}{2}}^{JT} E_{n.l.(o)} \tag{86}$$

where $E_{n.l.(o)}$ is the radial integral (see Eq. (26))

$$E_{n.l.(o)} = \langle^2 \pi \int_0^\infty r^2 dr (\sigma^4 - 4 f_\pi \sigma^3) \ . \tag{87}$$

To compute the quadratic and the quartic terms in the pion field the following property involving the coherent states $|\Pi_1\rangle$ and $|\Pi_2\rangle$ is very useful:

$$\langle\Pi_1| \ : \ \pi_j^n \ :|\Pi_2\rangle = [\frac{\langle\Pi_1|\pi_j|\Pi_1\rangle + \langle\Pi_2|\pi_j|\Pi_2\rangle}{2}]^n \langle\Pi_1|\Pi_2\rangle \ . \tag{88}$$

The quadratic term becomes

$$h^{JT}_{n.l.(\pi^2)} = e^{-N_\pi} \frac{2J+1}{2} \frac{2T+1}{2} \frac{1}{2} (F^{JT} + G^{JT}) E_{n.l.(\pi^2)} \ , \tag{89}$$

where the projection coefficient is now expressed in terms of (67) and (78), and $E_{n.l.(\pi^2)}$ is the radial integral

$$E_{n.l.(\pi)} = \frac{2\pi\lambda^2}{3} \int_0^\infty r^2 dr \phi^2 (\sigma^2 - 2 f_\pi \sigma) \ . \tag{90}$$

The evaluation of the quartic term is lengthy but straightforward, leading to

$$h^{JT}_{n.l.(\pi^4)} = e^{-N_\pi} \frac{2J+1}{2} \frac{2T+1}{2} E_{n.l.(\pi^4)} I^{JT} \ , \tag{91}$$

where $E_{n.l.(\pi^4)}$ is the mean field energy

$$E_{n.l.(\pi^4)} = \frac{\pi\lambda^2}{5} \int_0^\infty r^2 dr \phi^4 \tag{92}$$

and the projection coefficient is

$$I^{JT} = \cos^2\delta \ I_N^{JT} + \sin^2\delta \ I_\Delta^{JT} \ . \tag{93}$$

The functions I_N^{JT} and I_Δ^{JT} are defined by the integrals

$$\begin{aligned} I_N^{JT} &= \int_0^\pi \sin\beta d\beta \int_0^\pi \sin\beta_T d\beta_T \, d^J_{\frac{1}{2}\frac{1}{2}}(\beta) d^T_{\frac{1}{2}\frac{1}{2}}(\beta_T) e^{N_\pi \cos\beta \cos\beta_T} \\ &\cdot \ d^{\frac{1}{2}}_{\frac{1}{2}\frac{1}{2}}(\beta) d^{\frac{1}{2}}_{\frac{1}{2}\frac{1}{2}}(\beta_T) \frac{1}{8} \left[1 + \frac{1}{3}(1+\cos^2\beta)(1+\cos^2\beta_T) + 4\cos\beta\cos\beta_T \right] \ , \end{aligned} \tag{94}$$

and

$$\begin{aligned} I_\Delta^{JT} &= \int_0^\pi \sin\beta d\beta \int_0^\pi \sin\beta_T d\beta_T \, d^J_{\frac{1}{2}\frac{1}{2}}(\beta) d^T_{\frac{1}{2}\frac{1}{2}}(\beta_T) e^{N_\pi \cos\beta \cos\beta_T} \\ &\cdot \ d^{\frac{3}{2}}_{\frac{1}{2}\frac{1}{2}}(\beta) d^{\frac{3}{2}}_{\frac{1}{2}\frac{1}{2}}(\beta_T) \frac{1}{8} \left[1 + \frac{1}{3}(1+\cos^2\beta)(1+\cos^2\beta_T) + 4\cos\beta\cos\beta_T \right] \ . \end{aligned} \tag{95}$$

As for the functions defined by (68,69,79,80) the best way to compute (94,95) is by power series expansion of the exponential.

IV.3 Projection from the mean field and sum rules

The energy (45) of the state with angular momentum J and isospin T is given by

$$E^{JT} = E_0 + E_{n.l.(o)} + E_\pi \mathcal{C}^{JT} + E_{q\pi} \mathcal{C}_1^{JT} + E_{n.l.(\pi^2)} \mathcal{C}_2^{JT} + E_{n.l.(\pi^4)} \mathcal{C}_4^{JT} \tag{96}$$

with the new projection coefficients given by

$$\mathcal{C}_0^{JT} = \frac{G^{JT}}{F^{JT}}, \quad \mathcal{C}_1^{JT} = \frac{T^{JT}}{F^{JT}}, \quad \mathcal{C}_2^{JT} = \frac{1}{2}(1 + \mathcal{C}_0^{JT}), \quad \mathcal{C}_4^{JT} = \frac{I^{JT}}{F^{JT}}. \tag{97}$$

From the mean field results (Section III) the energy (96) can be computed. The procedure is clear: from the radial profiles the radial integrals denoted by E_α in (96) are computed from (73,77,83,87,90,92); the 'intrinsic number of pions' is calculated from (61); for this value of N_π and the mixing angle δ used to solve the mean-field equations (32- 35), the projection coefficients (97) are evaluated from (67,78,93). If one uses the value $\delta = 35.26°$ corresponding to the lowest mean field energy, the energy (96) is obtained in the so-called 'variation *before* projection' (VBP) method. In the next section we shall consider the 'variation *after* projection' (VAP)[16] which is conceptually superior, since for each projected state the radial functions and mixing angle δ are optimized. However, we may already consider here a partial variation after projection, namely on the variational parameter δ, to see whether it is possible to draw conclusions on the relevance of this degree of freedom.

Taking $g = 5.6$, for which the axial soliton is already stable, the mean field energy is $E_A = 1.55751$ GeV and the energies of the various states ($T = \frac{1}{2}, \frac{3}{2}; J$) are given in Table 1 (which refers to the nucleon) and Table 2 (which refers to the Δ) for fixed angle ($\delta = 35.26°$) and optimizing the angle for each state. Keeping δ fixed means that the various (J, T) components are being extracted from the same intrinsic state. In this case the probabilities (46) to find the state $|JT\frac{1}{2}\frac{1}{2}\rangle$ in the intrinsic axial state $|\psi_a\rangle$, which are given in Table 1 and 2, satisfy a sum rule (referred to below) and should add up to 1 (not exactly 1 since only a few states are considered in the Tables).

The comparison with experiment is postponed to the next section where a more reliable calculation is performed. From the values given in the Tables there is a non-negligible lowering of the energies when the mixing angle is varied for each projected state. Depending on the state, the mixing angle assumes values typically in the range $30° < \delta < 70°$, meaning that the inclusion of the bare delta state in the source is quite important. The nucleon energy is apparently too high in both methods but it will be lower when the better variational method is considered (next section). The number of pions in the projected state,

$$n_\pi^{JT} = \langle JTMM_T|n|JTMM_T\rangle \tag{98}$$

where n is the number of pions operator (see Eq. (60)), is given by an expression similar to the kinetic energy of the pions, i.e.

$$n^{JT} = N_\pi \mathcal{C}_0^{JT} \ . \tag{99}$$

For the nucleon states (Table 1) the projected number of pions is an increasing function of J, as expected. For the Δ channel (Table 2) the P_{33} state ($J = T = \frac{3}{2}$) contains less than one pion in the cloud due to the presence of the bare Δ in the source. All the other states contain more than one pion and, as expected, the higher the angular momentum the higher the number of pions.

Of particular importance in checking the formalism presented so far are the so-called sum rules. These are based on the fact that the intrinsic state can be expanded in angular momentum eigensates, $|\psi_A\rangle = \sum_{JT} a_{JT}|JT\frac{1}{2}\frac{1}{2}\rangle$, where $a_{JT}^2 = p^{JT}$ is given by (46). Sum rules are usually defined in percentage. The *Norm Weighted Sum Rule* is the sum of the probabilities times 100:

$$NWSR(\%) = 100 \sum_{J,T} p^{JT} \ . \tag{100}$$

The value 100% would be obtained if all (J, T) states were taken in the sum. In practice, however, one truncates the sum: for instance, in Tables 1 and 2 are included only states up to $J = 9/2$ and $J = 11/2$, respectively.

Nucleon State	VBP ($\delta = 35.26^{\circ}$)			VAP in δ	
J	Energy [GeV]	prob	$n_\pi^{J\frac{1}{2}}$	Energy [GeV]	$n_\pi^{J\frac{1}{2}}$
1/2	1.40058	0.46702	0.09106	1.13158	0.10934
3/2	1.84381	0.04954	1.12570	1.80346	1.14097
5/2	1.96510	0.02502	1.26986	1.95310	1.16264
7/2	2.63785	0.00127	2.28192	2.55872	2.17527
9/2	3.70441	0.00013	3.15576	3.69038	3.09128

Table 1: Energies and number of pions for different J states in the Nucleon ($T = 1/2$) channel. The radial fields were obtained in the mean field approximation for $g = 5.6$. For the *complete* variation before projection method, i.e. for the fixed angle $\delta = 35.26^{\circ}$, the probability of the projected state in the intrinsic state is also given.

Delta State	VBP ($\delta = 35.26^{\circ}$)			VAP in δ	
J	Energy [GeV]	prob	$n_\pi^{J\frac{3}{2}}$	Energy [GeV]	$n_\pi^{J\frac{3}{2}}$
1/2	1.84381	0.04954	1.12570	1.80348	1.14097
3/2	1.49841	0.30776	0.33273	1.49718	0.20557
5/2	2.17914	0.00939	1.67736	2.83910	1.51426
7/2	2.66839	0.00392	2.17364	2.66838	2.10184
9/2	3.52421	0.00011	3.24526	3.28419	3.15353
11/2	4.94808	0.00001	4.11717	4.93788	4.06550

Table 2: As in Table 1 for the Delta ($T = 3/2$) channel.

The *Energy Weighted Sum Rule* is defined by

$$EWSR(\%) = \frac{100}{E_A} \sum_{J,T} E^{JT} p^{JT} \ . \qquad (101)$$

This sum rule should be fulfilled if all states were considered in the sum, since the weighted average of the projected energies should then be equal to the unprojected energy E_A.

Finally we also considered a *Pion number Weighted Sum Rule* defined by

$$PWSR(\%) = \frac{100}{N_\pi} \sum_{JT} n_\pi^{JT} p^{JT} \ . \qquad (102)$$

The results for the Weighted Sum Rules in the complete VBP calculation (i.e. $\delta = 35.26^{\circ}$ and radial fields obtained from the mean field equations) and for coupling constant $g = 5.6$ are: $NWSR = 91.37\%$, $EWSR = 88.75\%$ and $PWSR = 72.20\%$. These figures get closer to 100% (i.e. the sum rules become almost exhausted), if the (unphysical) states with $T = \frac{5}{2}, \frac{7}{2}, ...$ are considered in expressions (100-102). From Tables 1 and 2 it is clear that the P_{11} and P_{33} states give the major contribution to the weighted sum rules.

V. Variation after projection

In the variation before projection method the radial functions and other variational parameters are determined requiring the energy of the mean field state to be minimal. In the variation after projection method, however, it is each projected energy that is minimized instead of the average energy, i.e. the radial functions and other variational parameters are optimized for each angular momentum and isospin eigenstate.

Conceptually the variation after projection method is better but it is much more difficult to implement.

Now the variational equations result from the variational principle $\delta E^{JT}/\delta\Omega_i = 0(\Omega_i = u, u, \phi, \sigma)$ subjected, in addition, to the restriction of normalization of the quark spinor. This variational principle leads to a set of four integro-differential equations whose numerical solution raises some technical difficulties. The energy (96) of an angular momentum and isospin eigenstate reads explicitly as

$$\begin{aligned} E^{JT} &= \int_0^\infty r^2 dr \left\{ 3\left[u\frac{dv}{dr} - v\frac{du}{dr} + 2\frac{uv}{r} + g f_\pi (u^2 - v^2) - g\sigma(u^2 - v^2) + \frac{2}{9} g uv\phi \mathcal{C}_1^{JT} \right] \right. \\ &+ 2\pi\left[\left(\frac{d\sigma}{dr}\right)^2 + m_\sigma^2 \sigma^2 \right] + \frac{2\pi}{3}\left[\left(\frac{d\phi}{dr}\right)^2 + 2\frac{\phi^2}{r^2} + m_\pi^2 \phi^2 \right] \mathcal{C}_0^{JT} \\ &+ \left. \pi\lambda^2 \left[\frac{\phi^4}{5}\mathcal{C}_4^{JT} + \frac{2}{3}\phi^2(\sigma^2 - 2f_\pi\sigma)\mathcal{C}_2^{JT} + \sigma^4 - 4f_\pi\sigma^3 \right] \right\} , \end{aligned} \tag{103}$$

which is similar to (26) except for the presence of the projection coefficients (97).

Due to technical difficulties, instead of the complete variation, we performed a restricted one in the spirit of the ideas put forward in Ref. [4]. Before explaining the algorithm in detail let us point out that the non-linear terms in the model Hamiltonian, resulting from the mexican-hat potential, although crucial to generate spontaneous breaking of the chiral symmetry and to allow for solitonic solutions in the model, do not give significant contributions to the total energy. Let us suppose, for a moment, that in the projected energy we set $\lambda^2 = 0$ (no mexican-hat), i.e., there are no non-linear terms. Then the pion sector of the linear sigma model reduces to the one considered in [4]. In such a case the function (see Eq. (59))

$$\xi(k) = \sqrt{\frac{2}{\omega_k}}\varphi_k \tag{104}$$

is given by the algebraic expression[4]

$$\xi(k) = -\frac{\alpha\tilde{\rho}(k)}{\omega_k(\omega_k + \Lambda)} \tag{105}$$

where $\tilde{\rho}(k)$ is a 'source function' and α and Λ are parameters. The mean field solution corresponds to $\alpha = 1$ and $\Lambda = 0$ and, even in the projected calculation, expression (105) still holds, but in such a case α and Λ are functionals of (105) itself. The mathematical problem seems difficult to be solved but, as pointed out in Ref. [4], α and Λ can then be treated as variational parameters which is technically much easier.

Coming back to the model with non linearities, the source radial function $\rho(r)$ contains a quark contribution (only a quantity corresponding to this one is present in [4]) and the (non-linear) pion contribution (see Eq. (35)):

$$\rho(r) = \frac{g}{2\pi} uvA(\delta) + \lambda^2\phi(\sigma^2 - 2f_\pi\sigma) + \frac{3}{5}\lambda^2\phi^3 \tag{106}$$

The source function $\tilde{\rho}(k)$ in k-space is just the transformed of $\rho(r)$ in r-space exactly as $\xi(k)$ in Eq. (59) is the transformed of $\phi(r)$.

In order to simplify the calculation, in Ref. [4] the variational parameter Λ was set to 0. We checked that this is fine for the P_{11} and P_{33} states in the sense that the energies of these states are not much dependent on Λ. For the other states the value $\Lambda = -m_\pi$ turns out to be a better choice since the energies become lower and we shall use this value here.

We proceed now in the following way. For a certain δ and coupling constant g the mean-field equations are solved, and the function (106) fixed; from $\rho(r)$ its transformed $\tilde{\rho}(k)$ is obtained which allows to construct (105) using, in the denominator, either $\Lambda = 0$ or $\Lambda = -m_\pi$, as already explained. Next the pion radial function in dependence of r is obtained taking the inverse of (59) i.e.

$$\phi(r) = \sqrt{\frac{2}{\pi}} \int_0^\infty k^2 dk j_1(kr)\xi(k) \qquad (107)$$

which depends explicitly on the variational parameter α. Given a value to this parameter, the intrinsic number of pions N_π is calculated from (61) and, using δ which was introduced at the very beginning, the projection coefficients (97) are also computed. The functions $u(r)$, $v(r)$ and $\sigma(r)$ are determined by solving numerically the system of three *differential* equations which follow from a variational principle for (103), assuming frozen $\phi(r)$, α and δ. These equations are

$$\frac{du}{dr} = [g(\sigma - f_\pi) - \epsilon]v + \frac{g}{9}\mathcal{C}_1^{JT}\phi u \qquad (108)$$

$$\frac{dv}{dr} = -\frac{2v}{r} + [g(\sigma - f_\pi) + \epsilon]u - \frac{g}{9}\mathcal{C}_1^{JT}\phi v \qquad (109)$$

$$\frac{d^2\sigma}{dr^2} = -\frac{2}{r}\frac{d\sigma}{dr} + m_\sigma^2\sigma - \frac{3}{4\pi}g(u^2 - v^2) + \lambda^2\left[\sigma^3 - 3f_\pi\sigma^2 + \frac{1}{3}(\sigma - f_\pi)\phi^2\mathcal{C}_2^{JT}\right] \qquad (110)$$

and, as for the mean-field case, the quark eigenvalue should be iterated until the quark normalization is achieved. Finally the projected energy (103) is computed. For a given mixing angle δ the variational parameter α is varied in order to find a minimum for the energy. The procedure is repeated until the energy minimum is found in the (δ, α) plane for each state.

Using the same model parameter as in the previous section, $g = 5.6$, the results are shown in Fig. 7 for the nucleon and in Fig. 8 for the delta channel. Plotted are the mass differences of the states with respect to the nucleon ground state. The energy of this state is $E^{\frac{1}{2}\frac{1}{2}} = 1.1147$ GeV and we checked that also the energies of the other states are always smaller than in the VBP calculation, as they should. The nucleon energy is still apparently high but one should keep in mind that the spurious energy associated with the centre-of-mass motion, which can be estimated in some 200 MeV [17], has not been removed. Hence, assuming that the spurious energy is about the same for all the states, in order to compare the results with the experimental data (indicated in the figures by open circles) it is more natural to plot just the mass differences rather than the absolute values. For the nucleon a reasonable agreement with data is obtained. For the delta such an agreement becomes poorer although one is still able to obtain the correct relative positions for the adjacent energy levels. These results do not get improved if an higher value of the coupling constant is considered. On the contrary, with a thicker pion cloud specially for high J, the theoretical prediction overestimates the data by larger amounts.

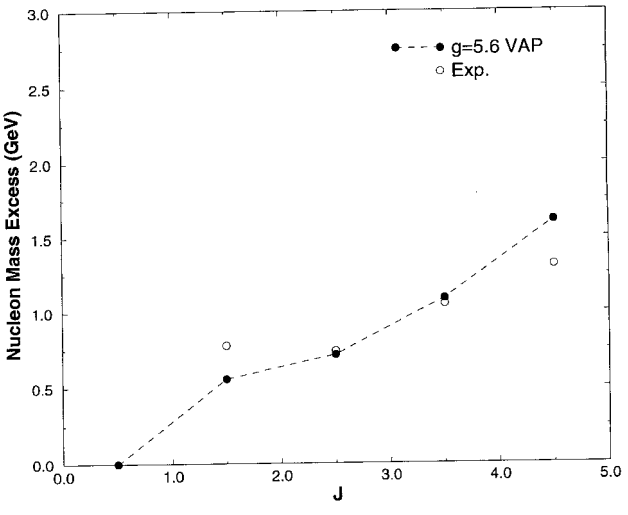

Figure 7. Comparison of the energy differences $E^{J\frac{1}{2}} - E^{\frac{1}{2}\frac{1}{2}}$ obtained in the model calculation with the experimental values, using an approximate variation-after-projection method (see text).

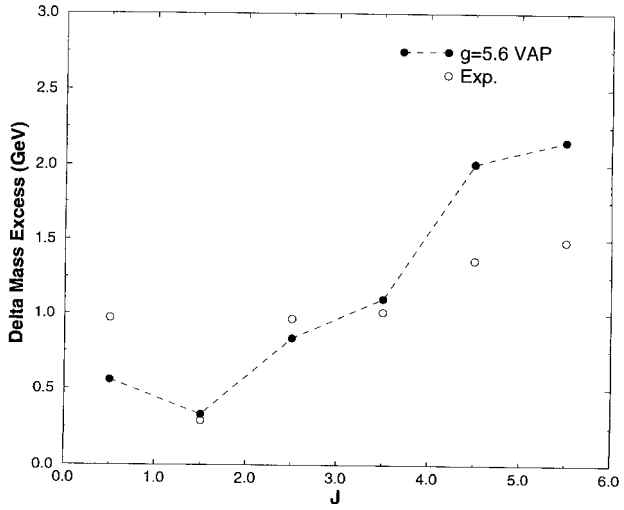

Figure 8. Comparison of the energy differences $E^{J\frac{3}{2}} - E^{\frac{1}{2}\frac{1}{2}}$ obtained in the model calculation with the experimental values, using an approximate variation-after-projection method (see text).

Apparently a thinner pion cloud would be desirable but for smaller g the soliton gets unstable (with respect to three free quarks) or does not exist at all. Probably better results could be obtained in the framework of the chromodielectric model which allows for chiral solitons where the quarks are confined by a chiral singlet field. Typically, in such models, the number of pion quanta in the cloud becomes considerably smaller with respect to the linear sigma model[18].

VI. Summary and conclusions

In this work we studied axial symmetric solutions of the linear sigma model. The axial symmetry refers to both configuration and isospin spaces. In a first step we considered just the mean field or, equivalently, classical solutions. The results are qualitatively similar to those found for the hedgehog, although the axial soliton is less bound than the hedgehog one. In order to describe physical states which are eigenstates of angular momentum and isospin we used the formalism proposed by Providência and Urbano based on a Peierls- Yoccoz projection from coherent states. The elegant mathematical formalism developed by those authors was extended in order to deal with the non-linearities of the model. In addition, we have considered a larger variational space which includes bare delta as well as bare nucleon states. The model prediction for the angular momentum excitations in the nucleon and delta isospin channel is reasonable in the first case but modest in the second one. The discrepancies are larger the higher the angular momentum. This is understandable, since for those states single particle quark excitations play an important role and these are not taken into account in our work. We remind that the linear sigma model only generates binding and not confinement and therefore the quark excitations lie in the continuum if the ground state has an energy around the nucleon mass. Finally, we stress that most of the expressions presented in this work may be used in a straightforward way in other quarks-meson models like chromodielectric and cloudy-bag like models.

Acknowledgement

Conversations with Enrique Ruiz Arriola are gratefully acknowledged. This work was partially supported by the Calouste Gulbenkian Foundation, Lisbon.

References

1. S. Kahana, G. Ripka and V. Soni, Nucl. Phys. **A 415**, 351 (1984); M. C. Birse and M. K. Banerjee, Phys. Lett. **B 136**, 284 (1984); Phys. Rev. **D 31**, 118 (1985).
2. B. Golli and M. Rosina, Phys Lett. **B 165**, 347 (1985); M. C. Birse, Phys. Rev. **D 33**, 1934 (1986).
3. M. Fiolhais, K. Goeke, F. Grümmer and J. N. Urbano, Nucl. Phys. **A 481**, 727 (1988).
4. J. da Providência and J. N. Urbano, Phys. Rev. **D 18**, 4208 (1978).
5. A. W. Thomas, Adv. Nucl. Phys. **13**, 1 (1983).
6. B. Golli, M. Rosina and J. da Providência, Nucl. Phys. **A 436**, 733 (1985).
7. J. N. Urbano and K. Goeke, Phys. Rev. **D 32**, 2396 (1985).
8. M. Fiolhais and M. Rosina, Portogal. Phys. **17**, 49 (1986).
9. R. E. Peierls and J. Yoccoz, Proc. Phys. Soc. London **A 70**, 381 (1957).
10. M. Fiolhais, J.N. Urbano and K. Goeke, Phys. Lett. **B 150** , 253 (1985).
11. E. Ruiz Arriola, P. Alberto, J. N. Urbano and K. Goeke, Z. Phys. **A 333**, 203 (1989).

12. M. Čibej, M. Fiolhais, B. Golli, M. Rosina, J. Phys. **G 18**, 49 (1992); L. Amoreira, M. Fiolhais, B. Golli and M. Rosina, J. Phys. **G 21**, 1657 (1995).
13. D. Ebert and H. Reinhardt, Nucl. Phys. **B 271**, 188 (1986).
14. G.E. Brown and W. Weise, Phys. Rep. **C 22**, 280 (1975).
15. J. Rafelski, Phys. Rev. **D 16**, 1890 (1977).
16. P. Ring and P. Schuck, *The Nuclear Many-Body Problem*, Springer-Verlag, New York, (1980) .
17. T. Neuber and K. Goeke, Phys. Lett. **B 281**, 202 (1992).
18. M. C. Birse, Progr. Part. Nucl. Phys. **25**, 1 (1990).